Leadership in Sustainable Infrastructure
Leadership en Infrastructures Durables

Vancouver, Canada
May 31 – June 3, 2017/ *Mai 31 – Juin 3, 2017*

VEHICLE DYNAMICS-BASED CIRCULATORY ROADWAY WIDTH OF SINGLE-LANE ROUNDABOUTS

Diachuk, Maksym [1] and Easa, Said 2[2,3]

[1,2] Ryerson University, Canada
[3] seasa@ryerson.ca

Abstract

Current guidelines for roundabout circulatory roadway width (CRW) are based on a static method that does not consider circulatory speed. In addition, the roundabout entry width is based on practical experience. This paper presents a method for determining the circulatory and entry widths based on a two-dimensional dynamic model that involves a system of differential equations. The method considers the interactions between the vehicle and the road geometric elements, including tire sideslip, vehicle weight, vehicle speed, and vehicle stability. The concept is illustrated using the intermediate semitrailer (WB-12) design vehicle. Design guidelines for the required circulatory width are established for different circulatory speeds (0-60 km/h) and different inscribed circle diameters (30-80 m). To simplify the guidelines, for each inscribed circle diameter, regression models were developed for the CRW as a power function of the circulatory roadway speed. The results show that the proposed method provides values of the CRW that are less than those of the current static method by 0.7-1.0. The proposed guidelines would be useful in case of space restrictions.

Keywords: roundabout, circulatory roadway width, vehicle dynamics, inscribed circle diameter.

1. INTRODUCTION

Geometric parameters of roundabouts are governed by the maneuvering requirements of the largest vehicles expected to travel through the roundabout. At single-lane roundabouts, the circulatory roadway width (CRW) should accommodate the design vehicle. Appropriate vehicle-turning templates or a CAD-based computer programs are normally used to determine the swept path of the design vehicle throughout the turning movements. Usually the left-turn movement is the critical path for determining the circulatory roadway width. According to AASHTO (2011), a minimum clearance of 0.6 m should be provided between the outside edge of the vehicle's tire track and the curb line. Gingrich and Waddell (2008) presented the required circulatory width for various inscribed circle diameters for different design vehicles. In some cases, particularly where the inscribed circle diameter is small or the design vehicle is large, the turning requirements of the design vehicle may dictate that the circulatory roadway be so wide that the amount of deflection necessary to slow passenger vehicles is compromised. In such cases, the CRW can be reduced and a truck apron, provided outside the mountable curb of the central island, can be used to accommodate larger vehicles.

The best known approach to swept path formulation is that of the Society of Automotive Engineers (SAE) (Kizas, 1997). Using this approach, the parameters of the circular movements for single and multiple unit vehicles have been established. This approach is static in nature and is mainly based on geometric relations

as the vehicle travels along the curve without considering the effect of vehicle speed. Thus, currently the circulatory width is determined using vehicle geometric interpretation either by the trigonometric functions of SAE method or using CAD procedures. The effect of vehicle dynamics behavior on the swept path at roundabouts has not been considered in previous research.

The purpose of this paper to present a dynamics-based model for determining roundabout CRW that considers vehicle speed at the steady-steady motion and illustrate its application for WB-12 design truck. The next sections present the experimental design and the vehicle dynamics model. The following sections present model validation and design guidelines for CRW for WB-12 design vehicle, followed by the conclusions.

2. VEHICLE DYNAMICS-BASED MODEL

The circulating roadway width is determined using vehicle swept path. To understand the phenomenon of swept path, it is essential to appreciate the significance of the various parameters affecting the turning behavior of a vehicle. The amount of swept path varies directly with the wheelbase length of a unit and inversely with the radius of the turn through which the vehicle travels. The magnitude of swept path is also affected by the number and location of the vehicle articulation points, the length of the arc negotiated during the turn, and vehicle speed.

In the dynamics-based model, the following assumptions are made: (a) a vehicle is assumed as plane, (b) the redistribution of longitudinal and transversal vertical reactions on vehicle wheels is neglected, and (c) the modeling of the contact forces between the tire and the road is based on the simplified Pasejka's magic formula for pure tire slip (Pacejka, 2002).

2.1 Model Description

Consider briefly the integration of motion equations, where an articulated vehicle is represented by a two-dimensional (2D) dynamic model (Figure 1). This dynamic model is different from the traditional system equations used in the state-space of the bicycle model for multiple unit vehicles (Ellis, 1969). The basic idea of the dynamic model is to account for the total number of tire contact points with the road surface and to use the matrix technique to represent model components. The model uses a minimum amount of necessary information that is optimally suited for fast computations in software packages such as MATLAB.

According to the principle of theoretical mechanics, consider a two-unit vehicle moving in a global coordinate system *XOY*. The vehicle is represented by massless rods pivotally jointed at point *P*. The distributed masses m_{TR}, m_{ST} and inertias I_{TR}, I_{ST} are concentrated at the physical centers of the units. The master unit is a tractor *TR* whose mass center is *C*, connected by a semitrailer *ST* whose mass center is *C'* (Figure 1). The masses are located at distances e_{TR}, e_{ST} relatively to the joint point *P*. In the process of angular motion the longitudinal axes of the tractor and semitrailer form an articulation angle, ψ.

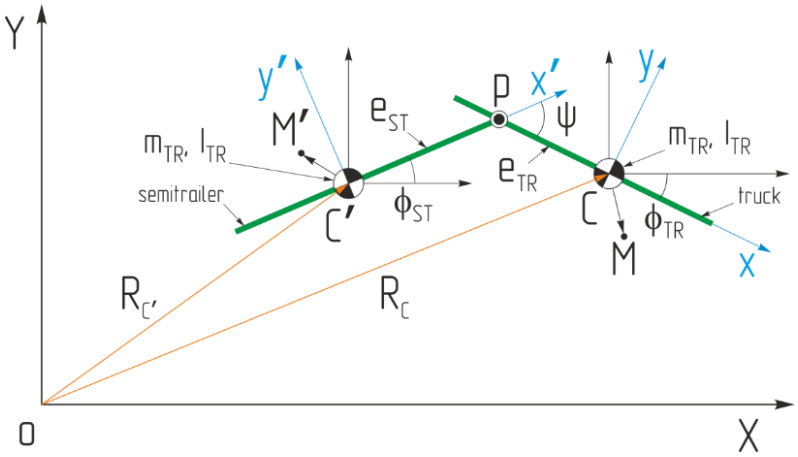

Figure 1 Schematic representation of articulated vehicle dynamics model

The vehicle's position at any time is sufficiently characterized by the combination of radii vectors (R_C and $R_{C'}$) from the origin of global coordinates to the unit mass centers. However, it is more convenient to use the generalized coordinates by introducing the mobile sub-global coordinate systems at the mass centers. The axes of the sub-global systems are parallel to the global system axes. The local coordinate systems *xCy* and *x'C'y'* (blue points in Figure 2) are introduced in the sub-global coordinate systems and can rotate around the centers *C* and *C'*, respectively. The equations of dynamics are composed relative to the sub-global coordinate systems. In addition, at any point *M* or *M'* additional sub-local coordinate systems could be input. For example, in the case of tires' points the systems are called wheels' coordinate systems (Pacejka, 2002), where the vectors of acting loads and forces are determined. Thus, the various degrees of freedom of the dynamics-based model are combined to form the vector (column matrix) *R*, as follows

[1] $$\boldsymbol{R} = \begin{pmatrix} X_{TR} \\ Y_{TR} \\ \phi_{TR} \\ \phi_{ST} \end{pmatrix};\ \boldsymbol{V_G} = \begin{pmatrix} V_{TR_X} \\ V_{TR_Y} \\ \omega_{TR} \\ \omega_{ST} \end{pmatrix};\ \boldsymbol{V} = \begin{pmatrix} V_{TR_x} \\ V_{TR_y} \\ \omega_{TR} \\ \omega_{ST} \end{pmatrix};\ \boldsymbol{J} = \begin{pmatrix} \dot{V}_{TR_x} \\ \dot{V}_{TR_y} \\ \dot{\omega}_{TR} \\ \dot{\omega}_{ST} \end{pmatrix};\ \boldsymbol{W} = diag \begin{pmatrix} \omega_{TR} \\ \omega_{TR} \\ \omega_{TR} \\ \omega_{ST} \end{pmatrix};\ \boldsymbol{F} = \begin{pmatrix} F_x^{(e)} \\ F_y^{(e)} \\ M_{TR_P} \\ M_{ST_P} \end{pmatrix}$$

where

X_{TR} = movement of tractor's mass center along the global axis *OX*;
Y_{TR} = movement of tractor's mass center along the global axis *OY*;
ϕ_{TR} = tractor's rotational angle relatively to the vertical axis passing through the tractor's mass center;
ϕ_{ST} = semitrailer's rotational angle relatively to the vertical axis passing through its mass center;
V_G = velocity vector in the global coordinate system according to the degrees of freedom;
V = vector of the main unknowns in the tractor's local mobile coordinates;
J = vector that characterizes the relative acceleration in the tractor's local coordinate system;
W = diagonal matrix of angular velocities ω_{TR}, ω_{ST};
F = vector of the generalized forces acting in the directions coinciding with the generalized coordinate system and reduced to the local coordinate system.

To obtain the motion equations, the fundamental theorems of theoretical mechanics regarding the changes of momentum and angular momentum are used. The impulse of the two-mass model $\vec{Q}_{\Sigma}$ is defined as

[2] $$\vec{Q}_{\Sigma} = \vec{Q}_{TR} + \vec{Q}_{ST} = m_{TR} \cdot \vec{V}_{TR} + m_{ST} \cdot \vec{V}_{ST}$$

where

$\vec{Q}_{TR}$, $\vec{Q}_{ST}$ = momentum vectors for the tractor and semitrailer, respectively
$\vec{V}_{TR}$, $\vec{V}_{ST}$ = absolute velocity vectors for the tractor and semitrailer mass centers, respectively.

The change of the mechanical system's momentum is caused by the action of the resultant of external forces, as follows

[3] $$\frac{d\vec{Q}_{\Sigma}}{dt} = \frac{d\vec{Q}_{TR}}{dt} + \frac{d\vec{Q}_{ST}}{dt} = m_{TR} \cdot \frac{\vec{V}_{TR}}{dt} + m_{ST} \cdot \frac{\vec{V}_{ST}}{dt} = \sum_k \vec{F}_{TR_k}^{(e)} + \sum_k \vec{F}_{ST_k}^{(e)}$$

where

$\vec{F}^{(e)}_{TR_k}$, $\vec{F}^{(e)}_{ST_k}$ = vectors of external forces acting at any point *k* of the tractor and semitrailer, respectively.

The first couple of scalar equations are obtained as the projections of the vector of Eq. (3) on the axes of the tractor's local coordinate system. To account for the rotational motion, consider the angular momentum change for each truck point M_k relative to the joint point *P*. Then,

[4]
$$\begin{cases} \sum_k \overrightarrow{PM_k} \times m_{TR_k} \cdot \dfrac{\vec{V}_{TR_k}}{dt} = \sum_k \overrightarrow{PM_k} \times \vec{F}^{(e)}_{TR_k} + \underbrace{\overrightarrow{PM_k} \times \vec{F}_P}_{\vec{0}} \\ \sum_k \overrightarrow{PM'_k} \times m_{ST_k} \cdot \dfrac{\vec{V}_{ST_k}}{dt} = \sum_k \overrightarrow{PM'_k} \times \vec{F}^{(e)}_{ST_k} + \underbrace{\overrightarrow{PM'_k} \times \vec{F}'_P}_{\vec{0}} \end{cases}$$

where m_{TRk}, m_{STk} = masses of point M_k of the tractor and semitrailer, respectively.

The internal forces at point *P* from the tractor and semitrailer, $\vec{F}_P$, $\vec{F}'_P$, respectively, produce no moments, unlike the external forces. Then, the generalized moments which acts on the tractor and semitrailer are, respectively, given by

[5] $$\boldsymbol{M}_{\boldsymbol{TR}_P} = \sum_k \vec{M}_{TR_P} = \sum_k \overrightarrow{PM_k} \times \vec{F}^{(e)}_{TR_k}; \quad \boldsymbol{M}_{\boldsymbol{ST}_P} = \sum_k \vec{M}_{ST_P} = \sum_k \overrightarrow{PM_k} \times \vec{F}^{(e)}_{ST_k}$$

Thus, the scalar equations of the second couple of rotational dynamics have been formed. Through simplification and transformation, the system of the second-order differential equations in vector-matrix format can be written as

[6] $$\boldsymbol{J} = \boldsymbol{M}^{-1} \cdot \left(\boldsymbol{F} + \left(\boldsymbol{L} + \boldsymbol{T} \right) \cdot \boldsymbol{W} \cdot \boldsymbol{V} \right)$$

Introducing auxiliary matrices for a more compact representation of Eq. (6), then

[7] $$\boldsymbol{Z}_2 = \begin{pmatrix} 0 & 0 \\ 0 & 0 \end{pmatrix}, \ \boldsymbol{E}_{2U} = \begin{pmatrix} 1 & 0 \\ 0 & 0 \end{pmatrix}, \ \boldsymbol{E}_{2L} = \begin{pmatrix} 0 & 0 \\ 0 & 1 \end{pmatrix}, \ \boldsymbol{D} = \begin{pmatrix} 0 & 1 \\ 0 & 0 \end{pmatrix}$$

[8] $$\boldsymbol{L} = \begin{pmatrix} \left(m_{TR} + m_{ST} \right) \cdot \left(\boldsymbol{D} - \boldsymbol{D}^T \right) & -m_{ST} \cdot e_{TR} \cdot \boldsymbol{E}_{2U} \\ -m_{TR} \cdot e_{TR} \cdot \boldsymbol{E}_{2U} & \boldsymbol{Z}_2 \end{pmatrix};$$

[9] $$\boldsymbol{T} = m_{ST} \cdot e_{ST} \cdot \left(\begin{pmatrix} \boldsymbol{Z}_2 & -\boldsymbol{D} \\ \boldsymbol{D}^T & \boldsymbol{Z}_2 \end{pmatrix} \cdot Cos(\psi) + \begin{pmatrix} \boldsymbol{Z}_2 & -\boldsymbol{E}_{2L} \\ \boldsymbol{E}_{2L} & -e_{TR} \cdot \boldsymbol{D}^T \end{pmatrix} \cdot Sin(\psi) \right).$$

It is more convenient to describe the matrix of inertia coefficients $\boldsymbol{M}$ as a sum of the constant part $\boldsymbol{M}_I$ and the variable trigonometric part $\boldsymbol{M}_T$,

[10] $$\boldsymbol{M} = \boldsymbol{M}_I + \boldsymbol{M}_T$$

where

[11] $$\boldsymbol{M}_I = \begin{pmatrix} \left(m_{TR} + m_{ST} \right) \cdot \left(\boldsymbol{E}_{2U} + \boldsymbol{E}_{2L} \right) & -m_{ST} \cdot e_{TR} \cdot \boldsymbol{D}^T \\ m_{TR} \cdot e_{TR} \cdot \boldsymbol{D} & I_{TR} \cdot \boldsymbol{E}_{2U} + \boldsymbol{E}_{2L} \cdot \left(I_{ST} + m_{ST} \cdot e^2_{ST} \right) \end{pmatrix}$$

[12] $$\boldsymbol{M_T} = m_{ST} \cdot e_{ST} \cdot \left(\begin{pmatrix} \boldsymbol{Z_2} & \boldsymbol{D} \\ \boldsymbol{D}^T & \boldsymbol{Z_2} \end{pmatrix} \cdot Sin(\psi) + \begin{pmatrix} \boldsymbol{Z_2} & -\boldsymbol{E_{2L}} \\ -\boldsymbol{E_{2L}} & e_{TR} \cdot \boldsymbol{D}^T \end{pmatrix} \cdot Cos(\psi) \right)$$

The transitions from the wheel, sub-local and local coordinate systems to the global coordinate system (which have a rotation angle ξ) are achieved through the following transition matrix,

[13] $$\boldsymbol{C}(\xi) = \begin{pmatrix} Cos(\xi) & -Sin(\xi) \\ Sin(\xi) & Cos(\xi) \end{pmatrix}$$

To transfer the velocities of the tractor's local coordinate system to the global coordinate system, the following matrix is formed,

[14] $$\boldsymbol{N}(\phi_{TR}) = \begin{pmatrix} \boldsymbol{C}(\phi_{TR}) & \boldsymbol{Z_2} \\ \boldsymbol{Z_2} & \boldsymbol{E_{2U}} + \boldsymbol{E_{2L}} \end{pmatrix}$$

Finally, using Eqs (1)-(14), the displacements are obtained using double integration, as follows

[15] $$\boldsymbol{V} = \int \boldsymbol{J} \cdot dt \; ; \; \boldsymbol{V_G} = \boldsymbol{N}(\phi_{TR}) \cdot \boldsymbol{V} \; ; \; \boldsymbol{R} = \int \boldsymbol{V_G} \cdot dt$$

The integration of acceleration and velocity of Eqs. (14) and (15) is carried out numerically in MATLAB using the solution method for stiff equation systems. Note that the power balance elements and simulation of tire-road contact are not demonstrated here due to sufficient prevalence of information.

The conversion of the generalized vehicle dynamics-based model from mathematics to animation is organized in several stages. First, according to vehicle geometric data an animation model is created that visually reflects a final solution of the dynamics equations and contributes to verifying the calculations. Second, the steering drive (a steering trapezoid in particular) are calculated and rationalized to provide accurate ratio of the steered wheels' turning angles (Ackerman's angles). Third, the masses and axial loads are distributed based on the weighting parameters. Finally, multiple calculations with any desired initial conditions are performed. Note that the dynamic model for a single-unit vehicle is a special case of the presented dynamic model of Eqs. (1)-(15), where one degree of freedom (slave unit) is removed.

2.2 Model Validation

The presented vehicle dynamics-based model, which considers the effect of circulatory speed, was first validated for WB-12 before establishing the design guidelines for the speed-based circulatory roadway width. The dimensions of the WB-12 design vehicles are shown in Figure 2. The validation is accomplished using three types of comparisons. First, the articulation angle of the dynamics-based model is compared with that of AASHTO. According to AASHTO (2011), during the U-turn execution with maximum steering rotation angle, the maximum articulation angle reaches a certain value. For WB-12, the articulation angle

reaches 46° at a maximum steering angle of 20.3°. The dynamics-based simulation of this maneuver with the specified conditions provided an articulation angle of 46.7°, indicating a relative error of 1.5%.

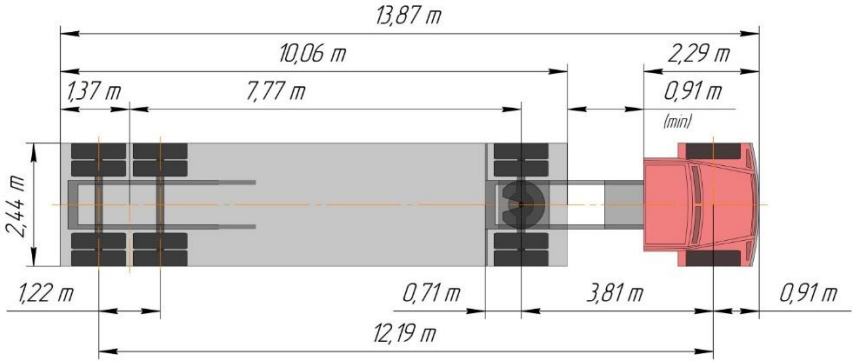

Figure 2 Design vehicles used in the study (AASHTO, 2011)

Second, the CRW of the dynamics-based model corresponding to the special case of a speed of practically zero (quasi-static model) is compared with that of the SAE geometric model, as shown in Table 1. The CRW was calculated for inscribed circle diameter of 30 m to 80 m. As noted, the maximum difference between the CRW of the quasi-static and geometric models is -0.1 m. Third, the CRW of the quasi-static model was compared with that of the AASHTO published values (Chan and Livingston, 2014).The ICD diameters were 33.1 m, 35.6 m, 40.8 m, and 50.0 m and the diameter values used for comparison were 35 m, 40 m, 45 m, and 50 m. The interpolated CRW values were 5.9 m, 5.7 m, 5.5 m, and 5.1 m. Comparing these values with those of the quasi-static case, the relative errors of the simulated CRW were -2.5%, -1.1%, 0.8%, and 3.0%, respectively.

In the preceding comparisons, a gross vehicle weight was assumed for the quasi-static case. To evaluate the effect of the vehicle weight on CRW, the CRW for an unloaded truck was calculated for different ICD values. The results showed that the resulting CRW were almost identical to those for loaded truck and the relative error was very small. Based on these results, the CRW will be established using the dynamics-based model with gross vehicle weight. The preceding results show that the special case of the proposed vehicle dynamics model (where the speed is practically zero) produces CRW values that are almost identical to those of the current static-based method. This close agreement provides evidence of the validity of the proposed method.

3. GUIDELINES FOR CIRCULATORY ROADWAY WIDTH

Consider the formation of the CRW on a single-lane roundabout for the three design vehicles (Figure 3). The figure shows the simulated steady-state movement at speed close to zero (quasi-static mode) and the movement on subcritical speed that precedes vehicle stability loss. For the quasi-static mode note that the planes of steered wheels are simultaneously perpendicular to the rays emanating from a turning center (Pacejka, 2002; Ellis, 1969).

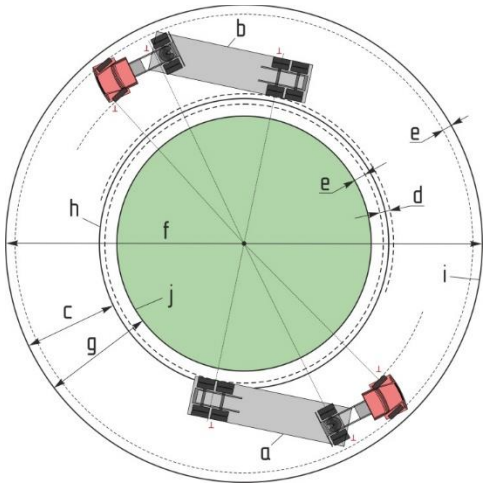

Figure 3 Formation of circulatory roadway width at single-lane roundabout for different design vehicles at quasi-static and steady-state dynamic modes (a = quasi-static movement mode, b = steady-state movement mode on pre-critical speed, c = remaining circulatory roadway width, d = maximum width difference, e = clearance from wheels (0.61 m), f = inscribed circle diameter (ICD), g = width between curbs (face to face), g' = width required for bus, h = low profile mountable curb at apron, i = inscribed circle, and j = central island).

The maximum difference in the CRW of the dynamics-based model substantially differ from those of the SAE geometric model depends on the circulatory roadway ICD and speed. The results show that the difference for for WB-12 lies in the range of 0.7 m (10.1%) to 1.0 m (19.2%) (Table 1). These results show that the CRW of the proposed dynamics-based model substantially differs from that of the SAE geometric model. To aid practical use the dynamics-based model, guidelines for CRW for WB-12 were established in the form of regression models and design charts. Regression models of CRW were established for each inscribed circle diameter as shown in Table 2. An example of the relation is shown in Figure 4.

Table 1 Comparison of geometric, quasi-static, and dynamics-based circulatory roadway widths [a]

Parameter	Inscribed circle diameter, ICD (m)										
	30	35	40	45	50	55	60	65	70	75	80
Calculated width for geometric model, m	6.9	6.2	5.8	5.5	5.3	5.2	5.0	4.9	4.8	4.7	6.9
Simulated width for quasi-static model (gross weight), m	6.9	6.3	5.9	5.6	5.4	5.2	5.1	5.0	4.9	4.8	6.9
Difference (geometric minus quasi-static models), m	0	-0.1	-0.1	-0.1	-0.1	0	-0.1	-0.1	-0.1	-0.1	0
Maximum difference (geometric minus dynamics-based models), m	0.7	0.8	0.9	0.8	0.9	1.0	0.9	0.8	0.9	0.8	0.7

[a] To convert from meter to feet multiply by 3.28

Table 2 Estimated regression models for dynamics-based circulatory roadway width [a]

Parameter	Inscribed circle diameter, ICD (m)										
	30	35	40	45	50	55	60	65	70	75	80
Speed, km/h	1-30	1-35	1-40	1-40	1-45	1-50	1-50	1-50	1-55	1-55	1-55
Coefficient ***a***, h·m/km, $\cdot 10^4$	-5.798	-3.316	-1.999	-2.325	-1.452	-0.792	-0.973	-1.137	-0.777	-0.763	-0.826
95% CB of ***a***,	-4.491	-2.055	-1.054	-1.387	-0.806	-0.261	-0.52	-0.696	-0.421	-0.437	-0.528

h·m/km, $\cdot 10^4$	-7.106	-4.577	-2.944	-3.263	-2.098	-1.322	-1.427	-1.577	-1.133	-1.089	-1.124
Coefficient ***b***	2.09	2.185	2.275	2.189	2.282	2.41	2.325	2.258	2.335	2.315	2.275
95% CB of ***b***	2.156 2.024	2.291 2.078	2.403 2.147	2.298 2.08	2.399 2.165	2.582 2.239	2.445 2.206	2.357 2.158	2.45 2.22	2.422 2.208	2.365 2.185
Coefficient ***c***, m	6.895	6.284	5.882	5.602	5.381	5.205	5.072	4.961	4.863	4.782	4.714
95% CB of ***c***, m	6.901 6.889	6.295 6.274	5.895 5.869	5.612 5.592	5.393 5.37	5.223 5.187	5.083 5.06	4.97 4.952	4.875 4.852	4.792 4.772	4.721 4.706

[a] R-square for all models is greater than 0.999.

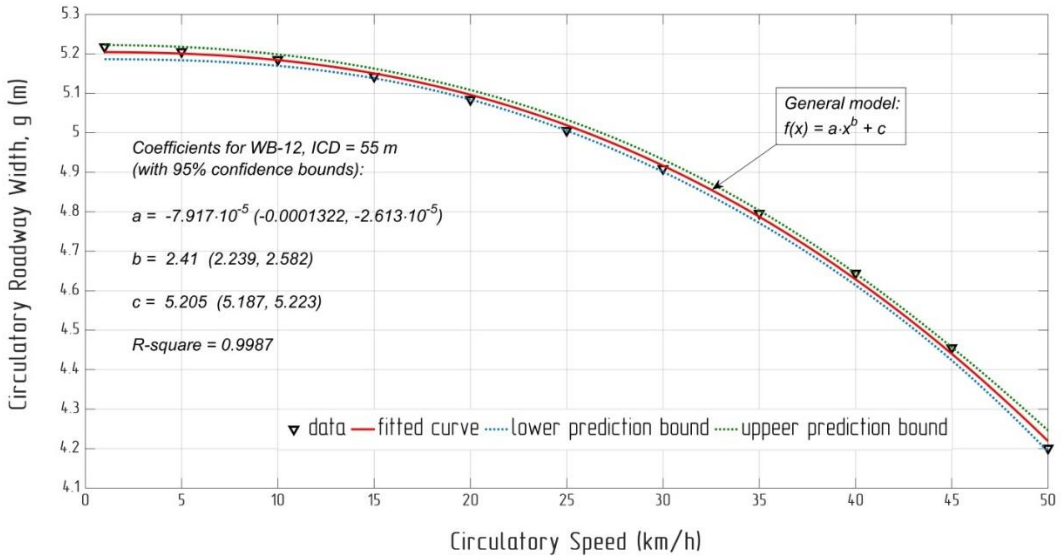

Figure 4 Example of regression relation between circulatory roadway width and speed for WB-12 design vehicle and ICD = 60 m

The circulatory roadway width is established as a function of speed for different inscribed circle diameters and different design vehicles, as shown in Figure 5. The ICD diameter varies from 30 (from 35 in the case of WB-20) up to 80 m with an increment of 5 m and the speed ranges from near zero (1 km/h), that provides simulation on quasi-static mode, to the critical speed which is limited by the conditions of vehicle motion stability (in speed increment of 5 km/h).

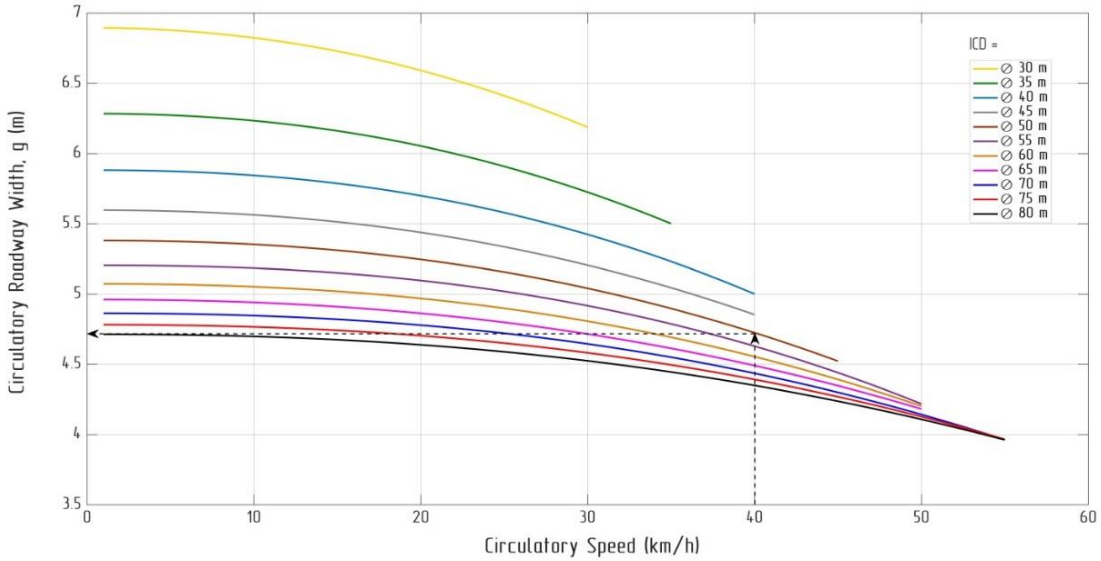

Figure 5 Design guidelines for roundabout circulatory roadway width using the dynamics-based

model for WB-12 design vehicle (for steady-state movement mode)

As an application example, consider a roundabout with an inscribed circle diameter of 50 m and circulatory roadway speed of 40 km/h. Determine the required width of the circulatory roadway based on the SAE geometric and proposed dynamics-based models. From Figure 5, the required CRW based on the SAE geometric model, which approximately corresponds to circulatory roadway speed of 1 km/h, is determined as 5.4 m. The CRW for the dynamics-based model, which corresponds to circulatory roadway speed of 40 km/h, is determined 4.8 m. Therefore, the actual CRW can be set as 4.8 m with the difference of 0.6 m (5.4 - 4.8) being used as part of a mountable area of the central island. This area will be used only in emergency or congested conditions, where the required CRW will be closed to 5.4 m.

4. CONCLUSIONS

This paper has presented a dynamics-based model for determining the circulatory roadway width of single-lane roundabouts. The model, which takes into account the effect of the circulatory roadway speed, provides lesser values of CRW than the SAE geometric model. Guidelines for CRW are established in the form of regression models and design charts for the WB-12 design vehicle. The results of the proposed dynamics-based model would be useful in situations in which space is constrained. It is recommended that the difference in the required CRW between the SAE geometric and dynamics-based models should be used as a mountable area of the central island. The presented guidelines are suitable for normal operations of the roundabouts. In case of emergency or traffic congestion, where the design vehicle will move at a low speed and requires a slightly larger circulatory roadway width, the design vehicle can use the mountable area of the central island.

ACKNOWLEDGMENT

The financial support of the Natural Sciences and Engineering Research Council of Canada (NSERC) is acknowledged.

REFERENCES

American Association of State Highway and Transportation Officials. 2011. *A Policy on Geometric Design for Highways and Streets*. AASHTO, Washington, D. C.

Chan, S. and Livingston, R. 2014. *Design Vehicle's Influence to the Geometric Design of Turbo-Roundabouts*. Transoft Solutions Inc., Richmond, British Columbia, Canada.

Ellis, J.R. 1969. *Vehicle Dynamics*. Business Books, London.

Gingrich, M. and Waddell, E. 2008. *Accommodating Trucks in Single and Multilane Roundabouts*. National Roundabout Conference, Kansas City, Missouri.

Infrastructure and Transportation, Motor Carrier Division 2016. *Vehicle Weights and Dimensions Guide: Vehicle Weight and Dimension Limits in Manitoba*. Website: www.gov.mb.ca/mit/mcd/ (accessed on December 15, 2016).

Kizas, J. 1997. *Design Vehicle Dimensions for Use in Geometric Design*. The technical report, Transportation Association of Canada, Ottawa.

Mathworks. 2016. MathWorks. Internet: www.mathworks.com/help/stateflow/ (accessed July 28, 2016)

Pacejka, H. B. 2002. *Tire and Vehicle Dynamics*. Butterworth-Heinemann, Amsterdam.

Rodegerdts, L. A. et al. 2010. *Roundabouts: An informational guide. National Cooperative Highway Research Program Report 672,* Transportation Research Board, Washington, D.C.

Saskatchewan Regulations. 2010. *Vehicle Weight and Dimension Regulations*. Saskatchewan, Regina.

Wikipedia. 2017. *Curb weight*. Internet: www.en.wikipedia.org/wiki/Curb_weight (accessed on December 15, 2016).